Rare Metal Materials and Engineering
Volume 46, Issue 2, February 2017
Online English edition of the Chinese language journal

Available online at www.sciencedirect.com
ScienceDirect

Cite this article as: Rare Metal Materials and Engineering, 2017, 46(2): 0355-0362.

ARTICLE

Effect of Stress-Aging Treatments on Precipitates of Pre-retrogressed Al-Zn-Mg-Cu Alloy

Xu Yongqian[1,2,3], Zhan Lihua[1,2,3], Li Shujian[1,2,3], Wu Xintong[1,2,3]

[1] Central South University, Changsha 410083, China; [2] State Key Laboratory of High-Performance Complex Manufacturing, Changsha 410083, China; [3] Collaborative Innovation Center of Advanced Nonferrous Structural Materials and Manufacturing, Changsha 410083, China

Abstract: According to retrogression and re-aging treatment (RRA), a novel retrogression and stress-aging treatment (RSA) was put forward for Al-Zn-Mg-Cu alloys. The effect of stress-aging time and external stress on precipitates of pre-retrogressed Al-Zn-Mg-Cu alloy was investigated by transmission electron microscope (TEM). The observation shows that there is a large number of matrix precipitates (MPts) and slightly discontinuous grain boundary precipitates (GBPs) in the pre-retrogressed alloy. The effects of stress-aging time and external stress on precipitates of the retrogressed alloy are significant. With the increase of stress-aging time and external stress, the size of MPts increases and the density of MPts decreases. Meanwhile, the size of GBPs, the distance between GBPs and the width of precipitate free zone (PFZ) increase. Compared with the traditional retrogression and re-aging treatment, the retrogression and stress-aging treatments increase the size of MPts, narrows the width of PFZ and make the GBPs more discontinuous for the studied Al-Zn-Mg-Cu alloy.

Key words: age forming; stress-aging; retrogression; precipitates; Al-Zn-Mg-Cu alloy

Stress aging is a combined thermal treatment in which an elastic stress is applied for creep age forming during artificial age-hardening of materials[1-3]. Al-Zn-Mg-Cu alloys are extensively used in aircraft fuselage, wing as well as other aircraft components, due to their very high strength and light weight[4,5]. One limitation of their use in the metallurgical state of highest strength (such as T6 or T651 temper) is the low resistance of these materials to structural corrosion[6]. A two-step heat treatment, retrogression and re-ageing (RRA), applied to Al-Zn-Mg-Cu alloys in the T6 temper has been shown to greatly enhance the SCC resistance of these materials with minimal tradeoff in strength[7,8]. According to RRA, a novel retrogression and stress-ageing treatment (RSA) is put forward. The fundamental purpose of RSA is to prove the feasibility of the collaborative of strength and corrosion resistance in creep age forming of pre-retrogressed Al-Zn-Mg-Cu alloys. Generally, the properties are related to microstructures, which are greatly influenced by the thermo-mechanical processing[9,10]. Therefore, it is very important to study the effects of thermo-mechanical processing on the microstructures of aluminum alloys.

In the past, the effects of creep age forming process on microstructures and properties of aluminum alloy have been paid attention to[11-16]. Among them, Jeshvaghani et al. [11, 12] investigated the effects of time and temperature on microstructure of the solution treated 7075 aluminum alloy sheet during creep age forming, and observed the evolution of matrix and grain boundary precipitates. Guo et al. [13] found that the external elastic tensile stress promotes the formation of precipitates and shortens the aging period of an Al-Zn-Mg-Cu alloy. Fribourg et al. [14] investigated the evolution of precipitate microstructure during creep of an AA7449 aluminum alloy, and found that plastic deformation applied at the aging temperature induces an

Received date: February 02, 2016
Foundation item: National Natural Science Foundation of China (51235010); National Key Basic Research Development Program of China (“973” Project) (2014CB046600)
Corresponding author: Zhan Lihua, Ph. D., Professor, College of Mechanical and Electrical Engineering, Central South University, Changsha 410083, P. R. China, Tel: 0086-731-88830254, E-mail: yjs-cast@csu.edu.cn

accelerated precipitate coarsening. It is noted that most of the above experimental materials are in the solution temper[11-13,15,16]. Comparatively, the stress aging behaviors of the aluminum alloys with different initial tempers have received less attention. Stress-aging behavior of aluminum alloy 2050 with different initial tempers (T34, T84 and as-quenched) has been experimentally investigated under both tension and compression stress-aging conditions by Y. Li et al [17]. Lin at el[18] studied the effects of pre-treatments on aging precipitates and corrosion resistance of a stress-aged 7050 aluminum alloy, and found that the density of aging precipitates first increases and then decreases with the increase of the retrogression time at 185 ℃. Meanwhile, the corrosion resistance of the stress-aged alloy after retrogression pre-treatment is greatly improved. Therefore, further investigations should be carried out to have a comprehensive understanding of the precipitation behaviors of Al-Zn-Mg-Cu alloy during the retrogression and stress-aging process.

In the present study, content stress aging tests of pre-retrogressed Al-Zn-Mg-Cu alloy were carried out over wide ranges of stress-aging time and external stress. The effects of stress-aging processing parameters on precipitates were discussed by the transmission electron microscope (TEM) observations. Also, the traditional RRA experiments have been carried out in order to compare the aging precipitation behavior between the RSA and RRA processes.

1 Experiment

The material used in the study is AA7B04, whose chemical composition is listed in Table 1. Fig.1 shows the retrogression and creep aging treatments procedures. The as-received material is T651 temper, which means the material has been solution-treated at 471 ℃ for 1 h, and water-quenched, followed by artificial aging treatment at 120 ℃ for 22 h and then 2% pre-stretched to remove residual stress and quench distortion. The bar specimen was designed for the retrogression and stress-aging tests, whose geometry is shown in Fig.2. The specimens were machined from the center of a 16 mm thick as-received plate along its rolling direction.

For retrogression pre-treatment[19,20], the as-received material was subjected to a retrogression heat treatment held at 180 ℃ for 20 min in a furnace, and water quenched to the room temperature. This state was called hereafter RHT (retrogression heat treatment).

Content stress-aging tests were carried out in a SUST-D5 creep testing machine with an assisting furnace. Two linear capacitance gauges were fitted onto the ridges of the specimen to measure the displacement during the tests. The 20 h stress-aging tests of the retrogressed AA7B04-T651 were carried out at stress levels of 90, 180 and 270 MPa.

Table 1 Chemical composition of 7B04 aluminum alloy (wt/%)

Zn	Mg	Cu	Fe	Si	Cr	Al
5.97	2.48	1.51	0.16	0.07	0.16	Bal.

Interrupted stress-aging tests, including 4 and 12 h were also carried out. All stress-aging tests were conducted at a temperature of 140 ℃ and the temperature was controlled within 2 ℃. During the tests, the load was applied after the temperature of the specimen reached a steady state of 140 ℃. After stress-aging test, the applied loading was released and the specimen was naturally cooled down to the room temperature in the furnace. This state, which underwent retrogression and stress-aging process, is called RSA for short. In addition, the traditional retrogression and re-aging process (RRA) at 140 ℃ of the 7B04-T651 aluminum alloy were also carried out to compare the aging precipitation behavior between the RSA and RRA processes.

The TEM specimens were prepared by cutting 3 mm diameter discs from the samples along the stress direction, thinning the discs mechanically to 0.08 mm after wards and then twin-jet-electro-polishing them to perforation with a mixture of 1/3 nitric acid and 2/3 methanol at –20 ℃, using a potential of 10 V. The prepared TEM specimens were examined on a Tecnai-F20 (200 kV) field-emission-gun transmission electron microscope (FEG-TEM).

2 Results and Discussion

The precipitates in aluminum alloy can be classified into three types in terms of the particle size. The first type is the coarse crystalline phase, which appears during the casting or solidification processes, and its size is usually above 1 μm. This type of precipitate is brittle, hence harmful to the fracture toughness of aluminum alloys. The second type is the dispersion which appears during the homogenization process. Its size is about 0.05~0.5 μm. The dispersion can inhibit recrystallization and grain growth. Due to the incohesion relationship between the precipitate and the aluminum matrix, the dispersion can induce transgranular fracture by the nucleation of voids. The third type is the aging precipitate, and its size is below 0.05 μm. Aging precipitate can strengthen aluminum alloys. Generally, this strengthening effect is decided by the morphology, modulus and interfacial or surface energy of the aging precipitates. It has been shown that the effects of the creep aging on the coarse constitute precipitates and dispersions are not obvious[21]. In the following sections, the effects of retrogression and stress-aging treatments on the aging precipitates will be investigated in detail.

2.1 Effect of retrogression heat treatment on aging precipitates

Fig.3 shows the TEM micrographs and corresponding select area electron diffraction (SAED) patterns of the AA7B04-T651 before and after retrogression heat treatment at 180 ℃ for 20 min. Fig.3a represents that the sample with T651 temper has abundant fine matrix precipitates (MPts) with the average size of 3.8 nm in aluminum matrix. Meanwhile, continuously distributed grain boundary precipitates (GBPs) are along with the grain boundary. Additionally, the average width is 14.8 nm for the precipitate free zone (PFZ). The presence of GPⅡ and η' phases in the aluminum matrix was established by analyzing SAD pattern as shown in Fig.3b. Compared to the microstructures of T651 state, it can be found that the density of the MPts in RHT sate is little reduced, the GBPs are slightly discontinuous and the width of PFZ is widened (Figs.3a and 3c). A similar result is found by Lin et al.[18]. From Fig.3d, the strong spots of GPⅡand η' phases and the weak spots of η phase can be seen in the retrogressed alloy. This indicates that the role of short-time retrogression treatment on the dissolution of precipitates is limited, namely only the MPts with size lower than a threshold size (i.e., GP zones and fine η' phases) can be dissolved.

2.2 Effects of retrogression and stress-aging treatments on transgranular precipitates

2.2.1 Effects of stress-aging time on transgranular precipitates

Fig.4 shows TEM micrographs and corresponding SAED patterns of the pre-retrogressed alloy under different aging time with stress of 180 MPa. The effects of stress-aging time on the size and distribution of MPts are significant. With the increase of stress-aging time, the size of MPts is increased and the density is decreased. After stress-aging at 140 ℃ for 4 h, the image contrast between the precipitates and aluminum matrix becomes evident (Fig.4a). The size of MPts in the 4 h creep-aged sample is larger than that in the as-retrogressed sample (Fig.4a and Fig.3b). The presence of GP zones, η' and η precipitates is established by analyzing SAED patterns of the pre-retrogressed alloy with various stress-aging time of 4, 12 and 20 h, as shown in Fig.4. It is indicated that the transformation GP zone into η' and η phases gradually occurs. Traditionally, the decomposition of supersaturated solid solution by precipitation is often considered in terms of three distinct steps: nucleation, growth and coarsening[22]. Simultaneously nucleation and growth is considered in the first stage of precipitation. During this initial stage, the density of precipitates is increased because new precipitates are nucleated. The mean precipitate size is given by the combination of the growth of existing precipitates and the arrival of new precipitates at the nucleation size. In the late stage of precipitation, the nucleation rate in the desaturated solid solution progressively decreases, and the alloy experiences a combination of growth and coarsening. Growth of the existing precipitates by diffusional transportation of atoms and coarsening, which involves the dissolution of small precipitates at the expense of large ones, is driven by an overall reduction in the interfacial energy[23]. In addition, the applied stress will produce abundant dislocations and promote the diffusion of atom/vacancy during stress-aging[24]. It can be deduced from Fig.4 that the studied alloy mainly experiences a combination of growth and coarsening mainly during the RSA process. Therefore, with the increase of creep aging time, the size of MPts increases and the density of MPts decreases.

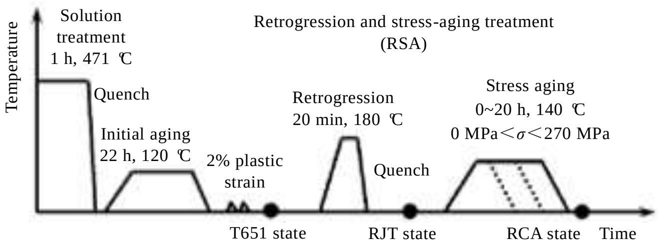

Fig.1 Retrogression and stress-aging treatment procedures

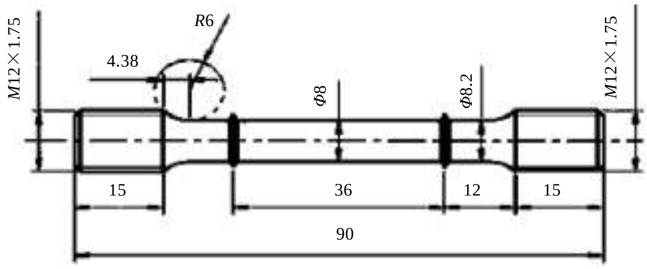

Fig.2 Geometry and size of sample (mm)

2.2.2 Effects of external stress on transgranular precipitates

The TEM micrographs and corresponding SAED patterns of the retrogressed AA7B04 under the stress-aging time of 20 h and different external stresses are shown in Fig.5. The effects of external stress on the growth and coarsening of the MPts are significant. When the external stress is 90 MPa, it can be found from Fig.5a that the main precipitates are η' phase and η phase. These precipitates are evenly distributed among the aluminum matrix. When the stress increases to 270 MPa, the coarse precipitates pointed by the black arrow occur, as shown in Fig.5b. It is indicated that the precipitation process is

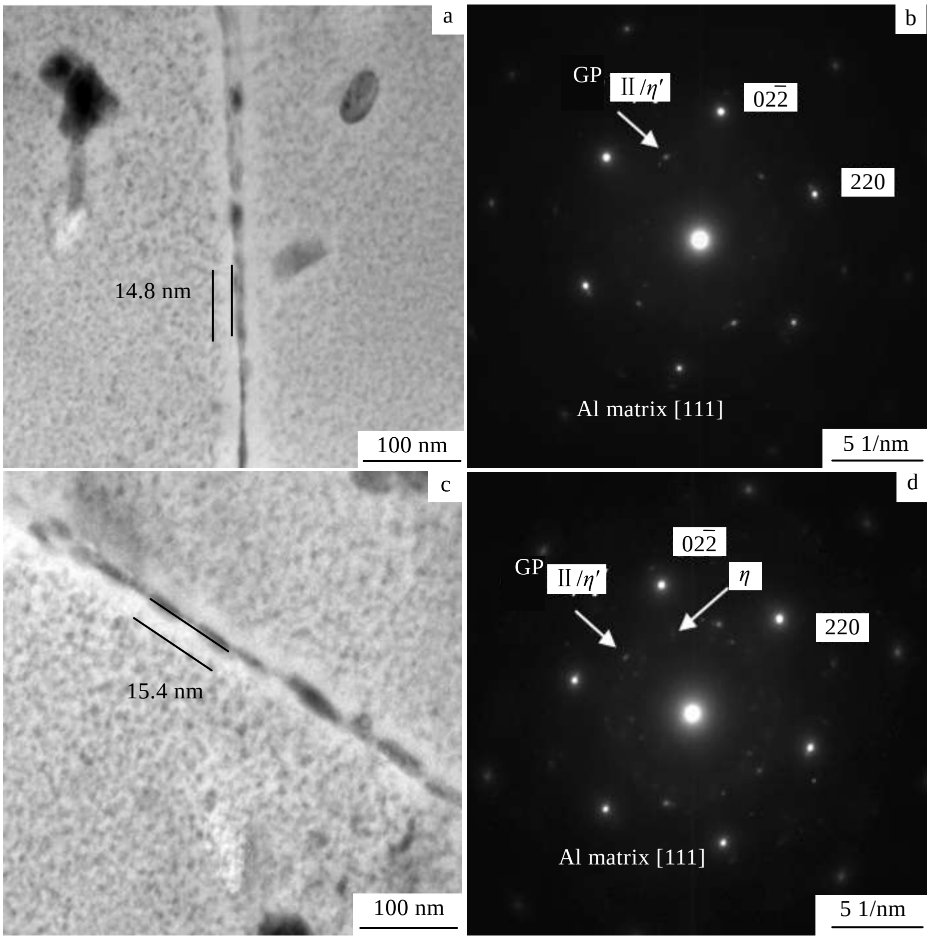

Fig.3 TEM micrographs (a, c) and corresponding SAED patterns (b, d) from <111>Al projection of the studied alloy before and after retrogression heat treatment: (a, b) T651 state, as-received material; (c, d) RHT state, 20 min heat treatment at 180 ℃

accelerated with the increase of external stress. Therefore, the size of MPts is increased and the density of MPts is reduced with increasing of external stress. Fig.5c shows the typical TEM micrograph of the RRA treated sample at the temperature of 140 ℃. It reveals that the precipitates with a mean size of 6.8 nm are homogeneously distributed in the aluminum matrix. However, the size of precipitates in the RRA treated sample is smaller than that in the RSA treated ones. Meanwhile, the density of precipitates of the RRA treated sample is larger than that of the RSA treated samples. According to the well-known LSW equation for coarsening kinetics[25], precipitate coarsening is mainly driven by the reduction of interfacial energy between precipitate and aluminum matrix. On one hand, the applied stress produces abundant dislocations and promotes the diffusion of atom/vacancy during stress-aging. On the other hand, these dislocation induced by creep deformation is attributed to a reduction of the interfacial energy between the precipitates and aluminum matrix[26]. Therefore, with the greater external stress levels, higher density of dislocations is generated with lower interfacial energy for coarsening, resulting in the larger size of MPts and the lower density of MPts during the retrogression and stress-aging tests for AA7B04-T651 alloy.

2.3 Effects of retrogression and stress-aging treatments on grain boundary precipitates

2.3.1 Effects of stress-aging time on grain boundary precipitates

Grain boundaries act as sinks of solute and vacancies, thus precipitate concentrating on the surroundings of this region. The growth and coarsening of grain boundary precipitates are accompanied by the formation of precipitate free zone (PFZ). Fig.6 presents the TEM micrographs of the pre-retrogressed alloy under the stress of 180 MPa and different stress-aging time. It can be found that the

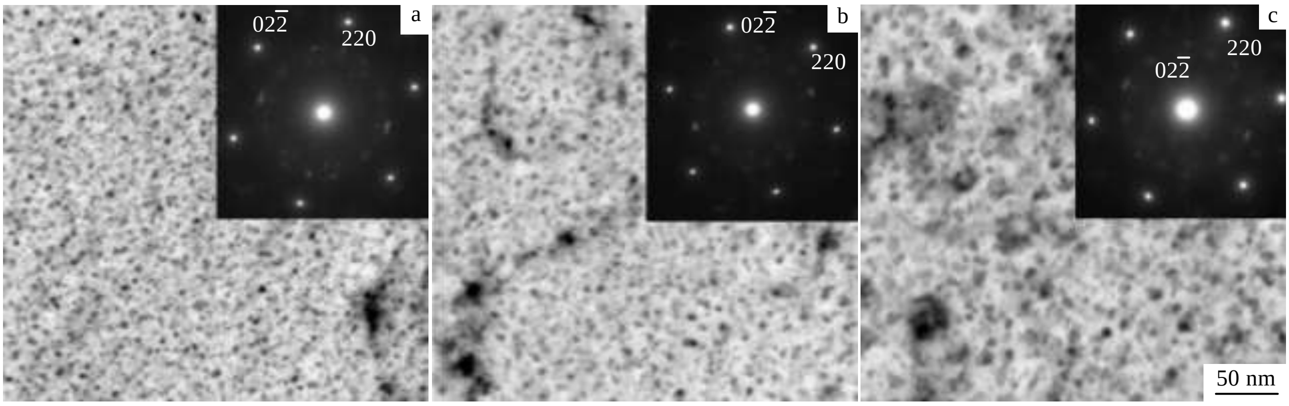

Fig.4 TEM micrographs and corresponding SAED patterns of the pre-retrogressed alloy under the external stress of 180 MPa and the stress-aging time of 4 h (a), 12 h (b), and 20 h (c)

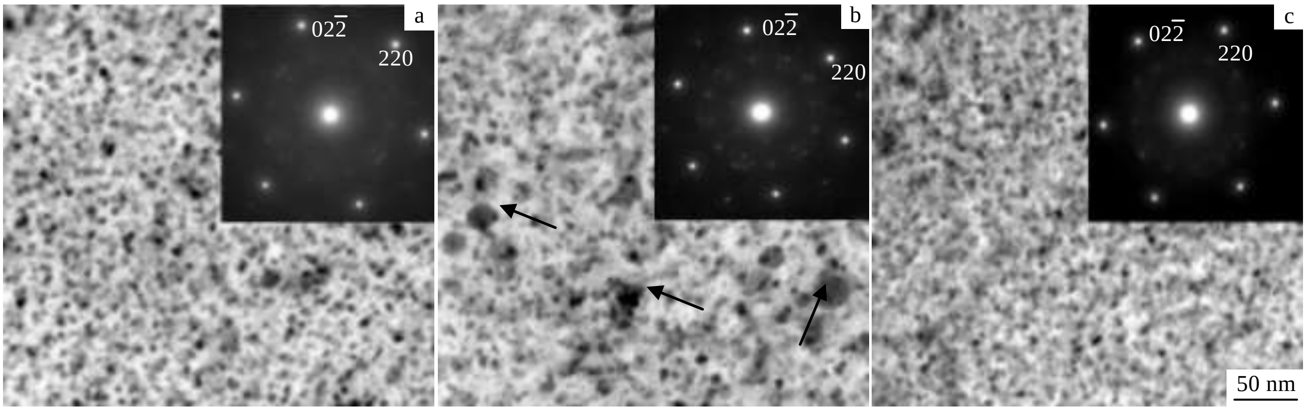

Fig.5 TEM micrographs and corresponding SAED patterns of the retrogressed alloy under the stress-aging time of 20 h and the external stresses of 90 MPa (a), 270 MPa (b), and 0 MPa (c)

increasing of stress-aging time can promote the distribution of the GBPs and increase the width of PFZ. After creep aging for 4 h, the GBPs are discontinuously distributed along the grain boundary, with a narrow PFZ of 15.6 nm in width. The width of PFZ in the 4 h creep-aged sample is wider than that in the as-retrogressed sample (Fig.6a and Fig.3b). Fig.6b and 6c shows the grain boundary microstructure of 12 h and 20 h creep-aged samples, respectively. With the increase of stress-aging time, the GBPs coarsen and concentrate quickly, and the width of PFZ increases. It has been shown that the outer atoms of MPts break away from nucleus and continuously spread to the grain boundaries with the increase of stress-aging time. Therefore, the unstable MPts dissolve, and the stable and coarse GBPs appear. Moreover, the average size of GBPs and the width of PFZ increase with the increase of stress-aging time. In addition, since the coarse GBPs take in a lot of solute atoms from its surroundings, the density of coarse GBPs decreases with the increase of stress-aging time.

2.3.2 Effects of external stress on grain boundary precipitates

Fig.7 shows the TEM micrographs of the retrogressed AA7B04 under different stress-aging stress levels for 20 h. From Fig.7a and 7b, it can be found that with the increase of external stress, the width of precipitate free zone increases from 21.6 nm to 23.1 nm. Meanwhile, the size of GBPs is obviously coarsened with increasing of external stress. Compared to the grain boundary microstructure in RRA treated sample, the width of the PFZ in RSA treated samples is significantly narrowed as shown in Fig.7c. Meanwhile, the distance between GBPs in the RSA treated sample is greater than that in the RRA treated sample. The precipitation process is likely to be affected by the elastic

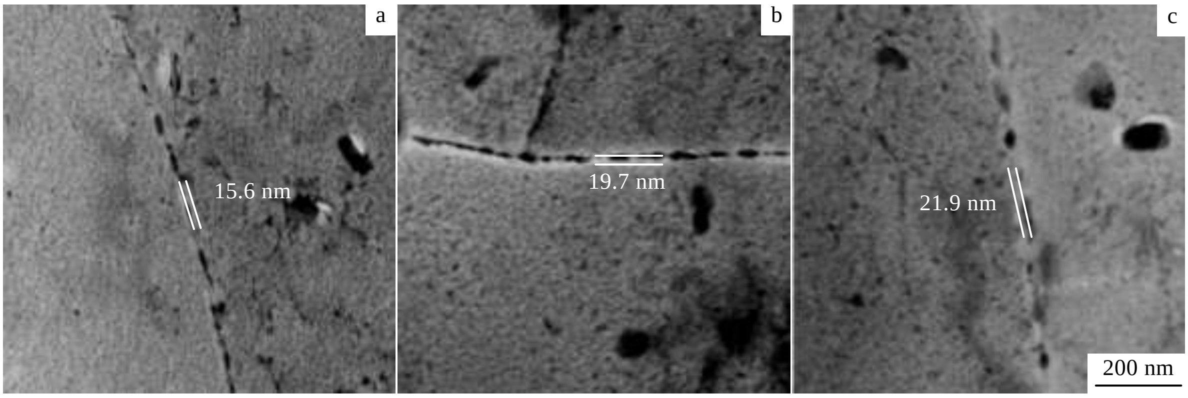

Fig.6 TEM micrographs of the retrogressed alloy under the external stress of 180 MPa and the stress-aging time of 4 h (a), 12 h (b), and 20 h (c)

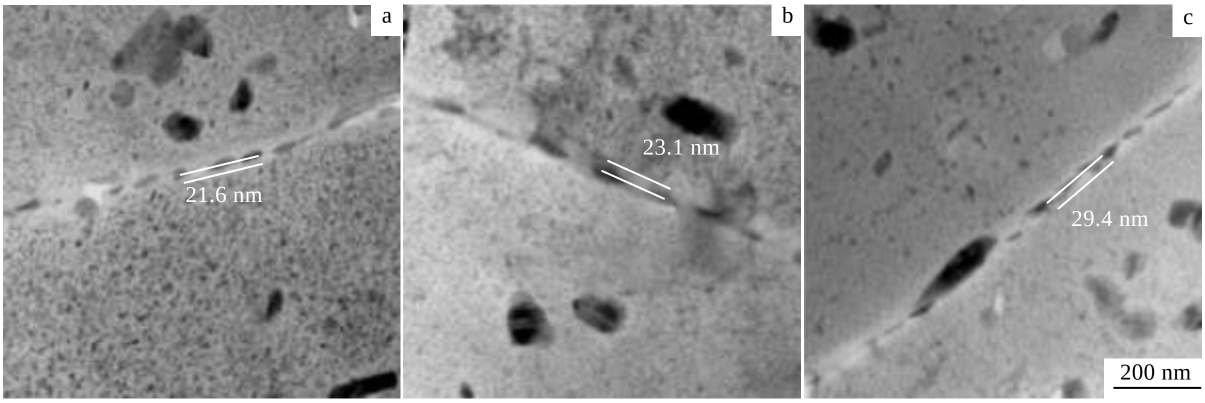

Fig.7 TEM micrographs of the retrogressed alloy under the stress-aging time of 20 h and the external stresses of 90 MPa (a), 270 MPa (b), and 0 MPa (c)

strain field of the beginning of stress-aging[27]. These dislocations are good for coarsening of the precipitates. Thus, the size of GBPs is increased with the increase of external stress. Lin et al.[21] has shown that the stress-aging process can produce an abundance of dislocations around the grain boundaries, which supplies the nucleation cores for MPts. For the RRA sample, there are few nucleation cores of MPts near the grain boundaries and the pre-existing GBPs grow up quickly during the aging process. Therefore, the PFZ width in RRA sample is larger than that in RSA samples.

The grain boundary microstructures can affect the corrosion resistance of aluminum alloys. It has been shown[28-30] that precipitate-free zones (PFZ) are the main paths for transgranular corrosion. Meanwhile, the dissolution of aluminum matrix occurs in the corrosion process of precipitate free zones. Grain boundary with continuous precipitates becomes a susceptive anode channel, which results in the galvanic reaction between the anodic precipitates and aluminum matrix. The potential difference between the grain boundary precipitates and aluminum matrix leads to the anodic dissolution of the precipitation. Thus, the electrochemical corrosion rate decreases, and the corrosion resistance increases because of the discontinuously-distributed precipitates. Therefore, it is important to control the grain boundary precipitates and precipitate free zone. Su et al.[31] studied the mechanical properties, microstructure, exfoliation corrosion (EXCO), and intergranular corrosion (IGC) behaviors of the spray-formed 7075 aluminum alloy after T6, T73, retrogression (R), and re-aging (RRA) treatment, and found that the discrete GBP and wide PFZ can improve the elongation, the EXCO, and the IGC resistance of the AA7075 alloy. It suggested that the corrosion resistance of the pre-retrogressed Al-Zn-Mg-Cu alloy improves with the increase of stress-aging time and external stress.

3 Conclusions

1) There is a large number of matrix precipitates (MPts) and slightly discontinuous grain boundary precipitates (GBPs) in the retrogressed alloy Al-Zn-Mg-Cu with heat treatment at 180 ℃ for 20 min.

2) With the increase of the stress-aging time and external stress, the density of dislocation increases and the interfacial energy decreases. Meanwhile, the size of MPts and GBPs is increased, the density of MPts and GBPs is decreased and the precipitate free zone (FPZ) is widened with the increase of the stress-aging time and external stress. It suggests that the corrosion resistance of the pre-retrogressed alloy improves with the increase of stress-aging time and external stress.

3) Compared with the retrogression and re-aging treatment, the retrogression and stress-ageing treatments increase the size of MPts, narrows the width of PFZ and makes the GBPs discontinuous.

References

1 Zhan Lihua, Lin Jianguo, Dean T A. *International Journal of Machine Tool Manufacture*[J], 2011, 51: 1

2 Lin Jianguo, Ho K C, Dean T A. *International Journal of Machine Tool Manufacture*[J], 2006, 46: 1266

3 Jeunechamps P P, Ho K C, Lin Jianguo *et al*. *International Journal of Mechanical Science*[J], 2006, 48: 621

4 Chen Gang, Chen Wei, Ma Li *et al*. *Rare Metal Materials and Engineering*[J], 2015, 44(9): 2120(in Chinese)

5 Su Xin, Liu Tan and Xu Guangming. *Rare Metal Materials and Engineering*[J], 2015, 44(3): 581 (in Chinese)

6 Marlaud T, Baroux B, Deschamps A *et al*. *Materials Science Forum*[J], 2006, 519-521: 455

7 Feng D, Zhang X M, Liu S D *et al*. *Materials & Design*[J], 2014, 60: 208

8 Li Zhihui, Xiong Baiqi, Zhang Yongan *et al*. *Transactions of Nonferrous Metals Society of China*[J], 2008, 01: 40

9 Li Bo, Pan Qinglin, Yin Zhimin. *Journal of Alloys and Compounds*[J], 2014, 584: 406

10 Zhang Hui, Jiang Fulin, Shang Xiaoyang *et al*. *Materials Science and Engineering A*[J], 2013, 571: 25

11 Jeshvaghani R A, Emami M, Shahverdi H R *et al*. *Materials Science and Engineering A*[J], 2011, 528: 8795

12 Jeshvaghani R A, Shahverdi H R, Hadavi S M M *et al*. *Materials Science and Engineering A*[J], 2012, 552: 172

13 Guo W, Yang M, Zheng Y *et al*. *Materials Letter*[J], 2013, 106: 14

14 Fribourg G, Bréchet Y, Chemin J L *et al*. *Metallurgical and Materials Transactions*[J], 2011, 42: 3934

15 Zhan Lihua, Li Yanguan, Huang Minhui. *Transactions of Nonferrous Metals Society of China*[J], 2014, 07: 2232

16 Li C, Wan M, Wu X D *et al*. *Materials Science and Engineering A*[J], 2010, 527: 3623

17 Li Y, Shi Z, Lin J *et al*. *Materials Science and Engineering A*[J], 2016, 657: 299

18 Lin Y C, Zhang J L, Liu G *et al*. *Materials Design*[J], 2015, 83: 866

19 Li Guofeng, Zhang Xinming, Li Penghui. *Rare Metal Materials and Engineering*[J], 2011, 40(7): 1295 (in Chinese)

20 Li Wenbin, Pan Qinglin, Liu Junsheng *et al*. *Rare Metal Materials and Engineering*[J], 2010, 39(9): 1646 (in Chinese)

21 Lin Y C, Jiang Y Q, Chen X M *et al*. *Materials Science and Engineering A*[J], 2013, 588: 347

22 Xu Xiaolong, Zhan Lihua, Li Yanguang *et al*. *Materials Science Technology*[J], 2013, 29(9): 1139

23 Robson J D. *Acta Materialia*[J], 2004, 52(15): 4669

24 Zhan L H, Lin J, Dean T A *et al*. *Journal of Mechanical Science* [J], 2011, 53: 595

25 Hillert Mats, Hunderi Ola, Ryum Nils *et al*. *Scripta Metallurgica* [J], 1989, 23(11): 1979

26 Zhu A W, Chen J, Starke E A *et al*. *Acta Materialia*[J], 2000, 48(9): 2239

27 Lin Y C, Xia Yuchi, Jiang Yuqiang *et al*. *Materials Science and Engineering A*[J], 2013, 565: 420

28 Oliveira A F, Barros M C, Cardoso K R *et al*. *Materials Science and Engineering A*[J], 2004, 379: 321

29 Xiao Y P, Pan Q L, Li W B *et al*. *Materials Design*[J], 2011, 32: 2149

30 Sun X Y, Zhang B, Lin H Q *et al*. *Corrosion Science*[J], 2013, 77: 103

31 Su Ruiming, Qu Yingdong, Li Rongde. *Journal of Materials Engineering and Performance*[J], 2014, 23(11): 3842

蠕变时效制度对回归态 Al-Zn-Mg-Cu 合金析出相的影响

徐永谦[1,2,3]，湛利华[1,2,3]，李树健[1,2,3]，吴欣桐[1,2,3]

(1. 中南大学，湖南 长沙 410083)

(2. 高性能复杂制造国家重点实验室，湖南 长沙 410083)

(3. 有色金属先进结构材料与制造协同创新中心，湖南 长沙 410083)

摘　要：基于回归再时效（RRA）工艺，提出一种新的回归－应力时效制度（RSA）用于Al-Zn-Mg-Cu合金。系统研究了应力时效制度(时效时间和应力)对回归态Al-Zn-Mg-Cu合金析出相的影响。透射电镜（TEM）观察结果表明：在回归处理后，合金内部存在大量的基体析出相（MPts）和轻微不连续的晶界析出相（GBPs）。时效时间和应力对回归态合金析出相的影响十分显著。随着时间和应力的增加，基体析出相的尺寸增加而密度减少；同时，晶界析出相的尺寸、间距和无沉淀的宽度也增加。相比于回归再时效工艺，回归-应力时效工艺使得晶内析出相尺寸增加，无沉淀析出带变窄且晶界析出相更不连续。

关键词：应力时效；回归处理；析出相；Al-Zn-Mg-Cu 合金

作者简介：徐永谦，男，1988 年生，博士，中南大学机电工程学院，湖南 长沙 410083，电话：0731-88830254，E-mail: 420575594@qq.com